ELSEVIER

Surface Science 373 (1997) 56–66

surface science

Hydrogen and oxygen negative ion production by surface ionization using diamond surfaces

P. Wurz *, R. Schletti, M.R. Aellig

Physikalisches Institut, University of Bern, Sidlerstrasse 5, CH-3012 Bern, Switzerland

Received 20 June 1996; accepted for publication 6 September 1996

Abstract

In this paper we report on the first observation of the formation of negatively charged ions upon reflection from a diamond surface. Positive H_2 and O_2 ions are scattered at small angles of incidence from a polycrystalline diamond surface. Charge exchange is observed yielding neutral particles and negatively charged ions. The negative ion fractions in the reflected particle flux are 5.5% and 29% for hydrogen and oxygen, respectively. These high negative ion yields are maintained in a moderate vacuum environment (10^{-7} mbar) over weeks without further periodic reconditioning of the surface.

Keywords: Atom and molecule irradiation effects, Charge transfer, Ion–solid interaction

1. Introduction

For a mass spectrograph for low energy particles, designed to explore the two-dimensional structure of magnetospheric features on the IMAGE satellite mission [1], surface ionization was identified as the only viable ionization technique to have the potential to meet the requirements concerning ionization efficiency for the energy range of 10 eV to 1 keV within the limitations imposed by the resources (space, weight, power, etc.) available on a satellite [2]. It was concluded that the ionization efficiency should exceed 1%, should be uniform over large areas, and should exhibit good long-term stability. Surface ionization introduces new demands on the design of the mass spectrometer and requires the development of new analyzer elements with matched ion optical properties. An instrument meeting these demands has been described recently [3,4]. The main species of interest in magnetospheric research are H and O atoms.

In the past 15 years, surface ionization has been studied extensively for potential application in fusion plasma research. With this technique, ionization efficiencies of up to 67% in the energy range from several eV to about 1 keV [5–7] have been achieved, using low work function (WF) surfaces for converting neutral particles or positive ions into negative ions. The physical process of ionization after reflection is resonant charge exchange from the conduction band of the converter surface to the affinity level of the scattered particle [7].

In most applications of surface ionization so far, a metal surface has been used, where the work function of the surface was significantly reduced by the application of a monolayer or less of an alkali metal [8] or an alkaline earth metal [9].

*Corresponding author. Fax: +41 31 631 44 04; e-mail: wurz@soho.unibe.ch

0039-6028/97/$17.00
PII S0039-6028(96)01146-6

The application of this overlayer of metal usually involves a dispenser, which releases defined quantities of the metal upon heating. Since the alkali metal and to a lesser degree the alkaline earth metal surface are chemically very sensitive, they degrade even in good vacuum after some time, and regeneration of the converter surface at regular intervals is necessary for long-term operation. This regeneration of the converter surface involves heating of the surface to substantial temperatures to evaporate the adsorbates, and the alkali or alkaline earth metal overlayer. Then, a fresh alkali or alkaline earth metal layer is applied. In addition to surface heating, the handling of a dispenser introduces some complexity, such as monitoring the WF of the surface. Despite these experimental challenges, Cs/W(110) [10] and Ba/W(110) [11] converter surfaces can in principle be used on a space platform.

In parallel, we were looking for an alternative converter surface, where the regeneration of the surface would be easier or not necessary at all. Recently, a LiF(100) surface, a wide bandgap insulator, was successfully employed for surface conversion, and negative ion yields of up to 70% for oxygen were reported [12]. Unfortunately, LiF is not a very stable surface chemically, and the usable energy range of the LiF surface does not fit our needs. As a potential candidate for surface ionization, we studied a diamond surface, which is chemically inert and very stable and is also an insulator. The diamond surface proved to be well suited for surface ionization. In this paper we report the details of these measurements.

2. Experimental setup

An experiment to study surface ionization was built to investigate the suitability of various conversion surfaces for their application on a space platform [13]. To assess the applicability of surface ionization to space instrumentation, two important issues had to be investigated: (1) degradation of the converter surface due to residual gas, and (2) degradation of the converter surface due to intense UV radiation. In addition, the particle reflection properties, which are important for the ion–optical design of the satellite instrument, had to be studied. Our experiment was designed to address the above-mentioned issues and thus to identify a conversion surface which meets the stringent qualifications necessary for space research. The schematics of the experimental setup are given in Fig. 1.

The experiment consists of an ion source, a beam guiding system, a sample stage with housing and with an alkali dispenser unit (not used for this study), and a detection unit. All these units are contained in a single vacuum chamber pumped by a turbomolecular pump.

Ions are formed in an electron impact ion source (Nier type), with the intensity of the primary beam ranging from 0.1 to 2 pA, and are accelerated to energies from 100 eV to 3 keV. These ions are then deflected in a 90° cylindrical energy analyzer, with an energy width of the ion beam at the sample of $\Delta E/E = 1\%$ (FWHM). The energy analyzer focuses the ion beam on the entrance aperture of the sample housing. Two diaphragms limit the beam size to $\varnothing$ 1 mm and the beam divergence to 1°. The impact angle of the ion beam on the conversion surface can be chosen between 90° and 0° with respect to the surface normal. The reflected beam is recorded on a two-dimensional position-sensitive MCP detector ($\varnothing$ 40 mm) which floats on an adjustable high voltage. In front of the MCP detector, a retarding potential analyzer (RPA) with three grids is mounted. The detector unit, including the RPA, is shielded electrostatically, and can be rotated independently from the converter surface around the same axis. The outer grids of the RPA are grounded to shield the inner grid, which has a permanent bias to suppress positive ions. An additional grid in front of the MCP detector at a negative potential with respect to the MCP detector serves to reject secondary electrons originating from the converter surface. Using the two-dimensional information from the detector, an angularly-resolved conversion efficiency can be derived. In addition, angular scattering in the polar and azimuth directions is measured with the detector.

Located outside the vacuum chamber is a halogen lamp coupled to a monochromator, which provides monochromatic light of variable wave-

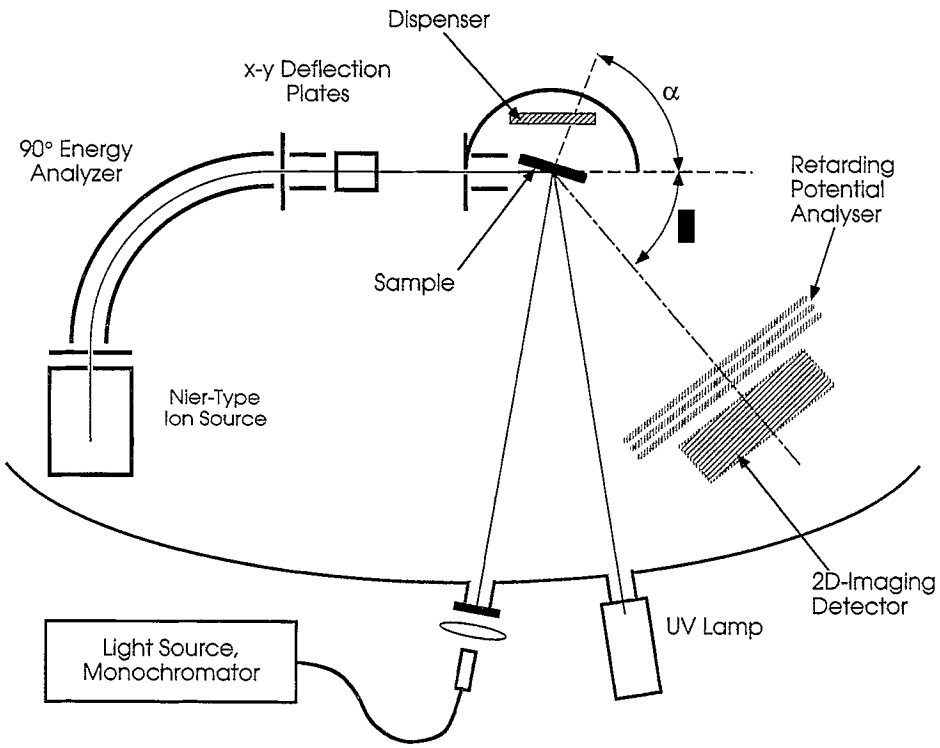

Fig. 1. Schematics of the experimental setup.

length for the work function measurement. This light is introduced into the vacuum chamber by a fiber-optical system and directed onto the conversion surface. The released photoelectrons are either measured with a pico-amperemeter attached to the sample or with the MCP detector. The latter is necessary when investigating an insulating surface. To test the UV response of the conversion surface, it can be exposed to very intense ultraviolet radiation produced by a QUANTATEC Xe lamp.

For the converter surface we used a silicon (100) wafer coated with polycrystalline diamond of 2 μm thickness [14]. The converter surface was stored in a container in air for several years before introduction into the vacuum. Our polycrystalline diamond sample has a mirror-like smooth surface with a grain size ranging from 10 to 100 nm, as verified by a SEM measurement. The surface was prepared in a manner suggested earlier [15,16]. The sample was washed in methanol immediately before being mounted in the vacuum chamber. After pump-down, the entire vacuum chamber was baked-out at 100°C for 24 hours, after which a residual gas pressure of 5×10^{-8} mbar was achieved. During operation the pressure may rise into the low 10^{-7} mbar range as a result of leaking the test gas into the ion source chamber. The surface was heated to approximately 500°C for a few minutes before a set of measurements was performed.

3. Results

Although we eventually want to use surface ionization to negatively ionize neutral atoms, for this experiment we used positive ions to investigate surface ionization. Furthermore, we used hydrogen and oxygen molecular ions rather than the respective atomic ions, because molecular ions can be produced far more efficiently in our system. The

impact of using positively charged molecular ions on the results is discussed in detail below.

The negative ion yield in the scattered beam is determined by measuring the total reflected beam and only its neutral component. The ionization efficiency η of the surface can be calculated from

$$\eta = 1 - \frac{N_0}{N_{tot}}, \quad (1)$$

where N_0 denotes the counts of the neutral portion of the reflected beam within a given detector area, and N_{tot} denotes the total counts within the same area and time. To sweep out negatively charged particles from the reflected beam, the MCP detector is floated on a high negative voltage with respect to the converter surface.

No reflected positive ions were detected in our experiment. Secondary electrons originating from the conversion surface and from the three RPA grids were hindered from reaching the MCP detector by a negative potential of 150 V on the entrance grid of the MCP detector. To identify further contaminations to our negative ion signal we performed measurements using Ne primary ions, which do not form negative ions. This result is used to modify Eq. 1. The final ionization efficiency of the surface is derived after corrections are applied to Eq. 1 accounting for the energy dependence of the detection probability and the different detector efficiencies for neutral particles and negative ions [11]. Applying all these corrections lowers the final negative ion yield compared to the measured number.

Fig. 2 shows the measured negative ion fraction in the reflected beam for H_2^+ primary ions in the energy range from 300 to 800 eV that were scattered from the polycrystalline diamond surface. After applying all corrections, the negatively charged fraction in the scattered flux is 5.5% at 400 eV and declines somewhat for higher energies. Because of the difference technique used for determining the negative ion fraction in the scattered flux, significant uncertainties are introduced as indicated by the error bars in Fig. 2. Fig. 3 shows the negative ion fraction in the reflected beam for O_2^+ primary ions in the energy range from 300 to 800 eV that were scattered from the polycrystalline

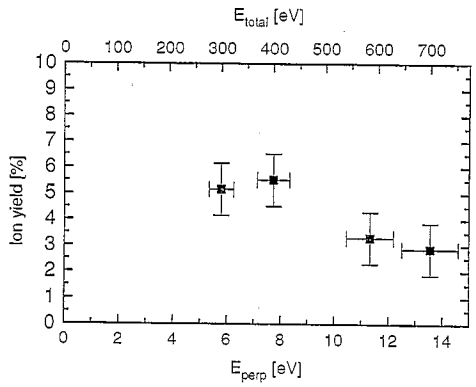

Fig. 2. Measured negative ion fraction in the scattered particle beam from a polycrystalline diamond surface for different primary energies for H_2 primary ions at an incoming angle of 82°. The entire scattered flux has been evaluated for this figure. The horizontal error bars only apply to the energy perpendicular to the surface, E_{perp}; the error in the total energy, E_{total}, is less than the symbol size.

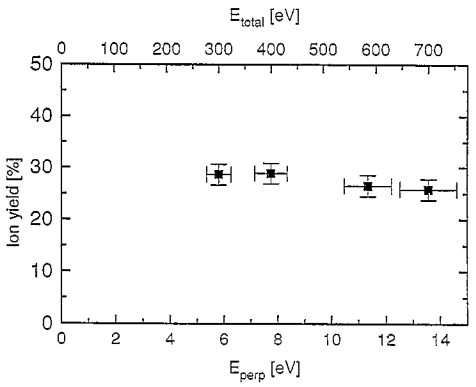

Fig. 3. Measured negative ion fraction in the scattered particle beam from a polycrystalline diamond surface for different primary energies for O_2 primary ions at an incoming angle of 82°. The entire scattered flux has been evaluated for this figure. The horizontal error bars only apply to the energy perpendicular to the surface, E_{perp}; the error in the total energy, E_{total}, is less than the symbol size.

diamond surface. After applying all corrections, the negatively charged fraction in the scattered flux is 29% at 300 eV and is almost constant with energy.

For hydrogen as well as for oxygen, we find that the ionization efficiency of the diamond surface remained constant for periods of weeks. Fig. 4 shows two sets of measurements of the negative

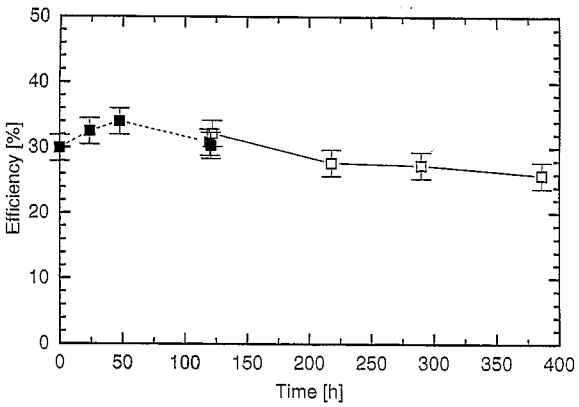

Fig. 4. Measured negative ion fraction in the scattered beam from a polycrystalline diamond surface for O_2 primary ions at 770 eV at 82° impact angle for extended time periods. The full symbols indicate the first set of measurements, the open symbols indicate the second set of measurements. Before each set of measurements the sample was heated to approximately 500°C.

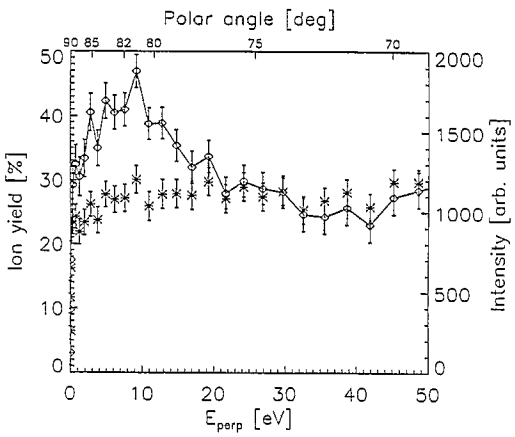

Fig. 5. The dependence of the negative ion yield (asterisk, left hand scale) on the energy perpendicular to the surface as it is evaluated from a measurement of O_2^+ at an energy of 770 eV and an incoming angle of 82°. The outgoing polar angle of the reflected ion is used to derive the energy perpendicular to the surface, whereby reflected atomic oxygen ions are assumed. The intensity of the scattered ion flux is overlaid (diamonds, right hand scale).

ion yield for O_2 primary ions for extended time periods demonstrating the long-term stability of the diamond surface. Within the uncertainties of the measurements, no degrading effect e.g. due to the background gas (in the low 10^{-7} mbar range) or due to the primary beam was observed. Initially, the diamond sample was heated before a set of measurements was started. However, later it was verified that this thermal cleaning is not necessary. A diamond sample was left in air before introduction into the vacuum chamber, and the reported ionization efficiencies were reproduced.

Fig. 5 shows the dependence of the negative ion yield on the energy component perpendicular to the surface of the reflected particles for an O_2^+ primary ion beam with an energy of 770 eV and an incoming angle of 82°. The outgoing angle of the reflected ion is used to derive the energy perpendicular to the surface, whereby reflected atomic oxygen ions are assumed. The intensity of the scattered particle flux is overlaid in Fig. 5, and shows a pronounced peak in specular direction, but also a pedestal extending to large polar angles. This feature probably comes from particle reflections at grain boundaries of our polycrystalline surface. Using single-crystal surfaces, we never observed such a pedestal. The negative ion yield is found to be mostly independent of the energy perpendicular to the surface. The modulation seen in Fig. 5 in the negative ion yield is caused by statistical variations due to the limited number of counts available for an angle bin. For small energies perpendicular to the surface (small polar angles), the negative ion yield drops gradually to zero.

The measured angular scattering in polar and azimuthal direction for a H_2^+ beam impinging on a diamond surface at an impact angle of 85° with an energy of 770 eV is displayed in the upper panel of Fig. 6. The measured angular scattering at FWHM was 15° in the azimuthal direction and 15° in the polar direction. These values are consistent with MARLOWE [17] computer simulations we performed. In the lower panel of Fig. 6 the angular scattering is shown for an O_2^+ beam at an impact angle of 87°. At this shallower angle of incidence a narrower specular peak and a reduced pedestal are observed.

To test the UV response of our diamond surface, we illuminated it with an intense UV lamp for a period of 75 hours. No adverse effect on the negative ion yield is observed. The intensity of the lamp is three times the intensity of the sun at the

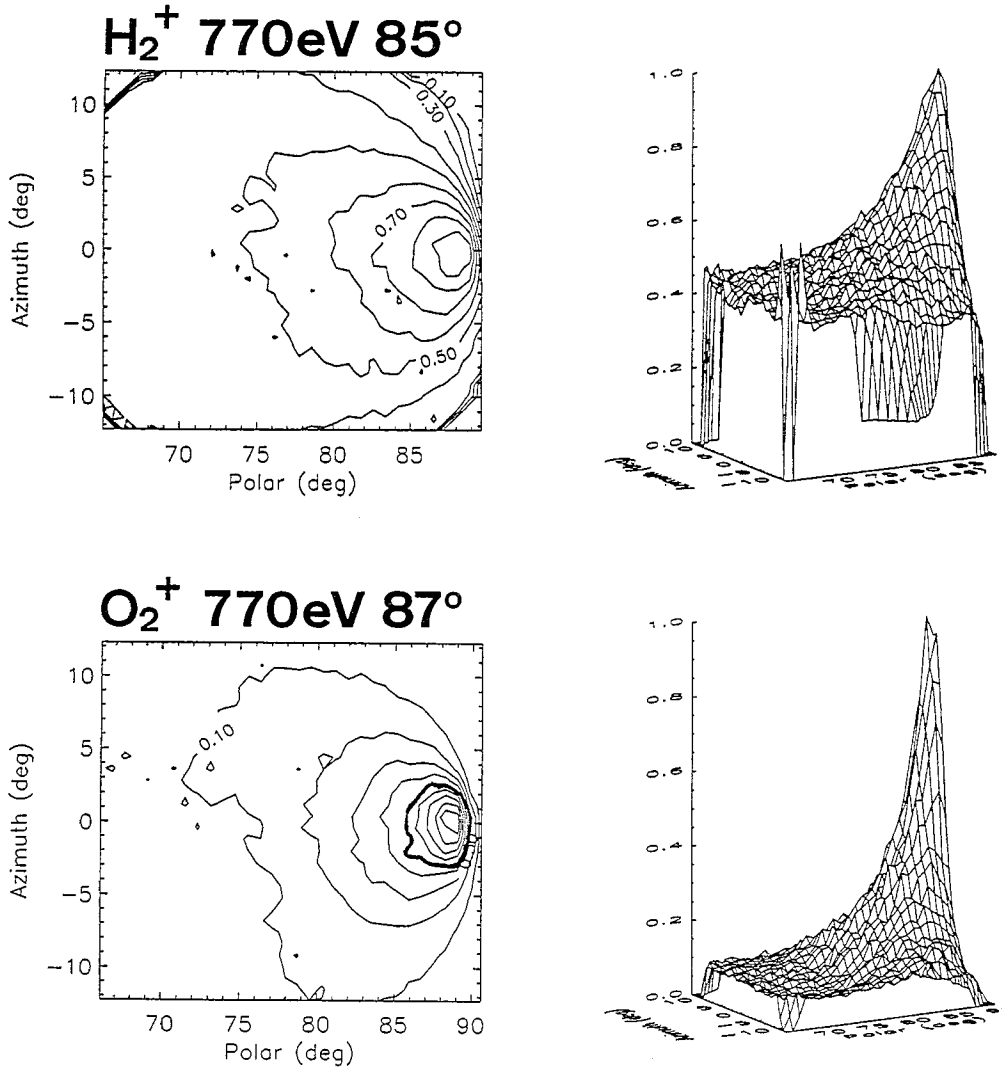

Fig. 6. Measured angular scattering in polar and azimuthal directions for an ion beam with an energy of 770 eV impinging on a diamond surface. Upper panel: H_2^+ at an angle of 85°, lower panel: O_2^+ at an angle of 87°.

location of the earth in the UV range below 150 nm; i.e. the conversion surface is irradiated with 2×10^{13} photons $s^{-1}\,cm^{-2}$, which compares to 6×10^{11} photons $s^{-1}\,cm^{-2}$ from the sun in this wavelength interval at the position of the earth [18]. From the geocorona a photon flux of 2×10^7 photons $s^{-1}\,cm^{-2}$ is expected on the conversion surface [10], given by the field of view of $10° \times 90°$ for the proposed instrument [3,4]. Also, in earlier work where we studied the UV degradation of Cs/W(110) and Ba/W(110) conversion surfaces, we did not find any indication of a degradation of the ionization efficiency with exposure to intense UV radiation [10,11].

4. Discussion

Incoming ions approaching a metallic surface are effectively neutralized via an Auger-type

electron transfer process or by a resonant electron transition [19,20]. As a result, using positive primary ions will not affect the determination of the ionization efficiency. This has been demonstrated experimentally by comparing ionization efficiencies for D^+ and D^0 primary particles [21].

The interpretation of the results is complicated by the fact that the hydrogen and oxygen molecules dissociate upon neutralization in front of the surface on the incoming part of the trajectory. In the case of hydrogen, two different ion states are involved in the charge exchange with the surface for the neutralization, one which is bonding ($b^3\Sigma_u^+$) and one which is anti-bonding ($X^1\Sigma_g^+$) [20]. Collisional dissociation can be ruled out as a relevant dissociation process for hydrogen, because the elastic energy transfer is too low at the energies and scattering angles used in our experiment [22,23]. From recently published data we estimate that the dissociation of hydrogen molecules when approaching the surface amounts to 80% in our experiment [22–24]. H^- and H_2^- ions are both detected in our measurements. Although H_2 only forms a metastable negative ion [25], its lifetime of $>10^{-5}$ s [26] exceeds the time for detection by an order of magnitude in our experiment. The measured negative ion yield represents the value for atomic hydrogen, because the flux impinging on the conversion surface consists mostly of neutral hydrogen atoms. This conclusion is in agreement with earlier measurements in the same energy range [25], where no difference in the negative ion yield was observed for primary H^+ or H_2^+ ions. The authors concluded that the incoming molecular hydrogen ions dissociate shortly before they hit the surface, leading to the reflection of two individual neutral hydrogen atoms. Using D_2^+ primary ions instead of D^+ ions, a small reduction in the negative ion yield was observed for low energies (<1 keV) [21], indicating that the yield of negative deuterium molecular ions is somewhat lower than for the negative atomic ion.

As with hydrogen, the oxygen molecule also dissociates upon neutralization when approaching the surface. The most likely mechanism is resonant electron capture into repulsive Π states, yielding oxygen atoms in the ^3P or ^1D states which then hit the surface. From measurements of oxygen molecules scattered from Ag(111) surfaces we estimate the dissociation to be around 80% at our energies [28]. The much larger valence bandwidth of diamond (21 eV) may mean that this estimate is too high, because the bound O_2 states can be populated by a resonant transition rather than an Auger transition. Again, collisional dissociation of the oxygen molecule can be ruled out for the same reasons as for the hydrogen molecule. Thus we can assume that the flux impinging on the conversion surface consists primarily of oxygen atoms and the measured negative ion yield represents the value for atomic oxygen. To verify this assumption we did one measurement using atomic oxygen ions. The result of this experiment gave a conversion efficiency which, within the measurement uncertainty, is in accordance with the results obtained for O_2 (Fig. 3). This agrees with the assumption that most of the molecules are dissociated before they hit the surface. The O_2^- ion is also detected in our system, because O_2 forms a stable negative ion with an electron affinity of 0.44 eV [29]. Once the internal energy of the molecular ion exceeds this value, O_2^- autodetaches with a lifetime of the order of 10^{-10} s.

We proceeded to estimate what effect the mixture of atomic and molecular particles has on the outcome of the measurement of the total ion yield [11]. By assuming the above-mentioned dissociation rates for the hydrogen and oxygen molecules, and knowing the detection efficiency for hydrogen and oxygen atoms and molecules and their respective negative ions for our detector, we get pairs of ion yields for the atomic and molecular ions for each measurement of the total ion yield. Since we don't know either value in the pair, we cannot determine the individual ion yields. However, the effect on the yield of atomic ions is small, since this is the majority component in the scattered flux. Most likely, the yield for atomic ions is a little bit higher than the total ion yield we measure.

In the following we will briefly review the existing theories dealing with the formation of negative ions upon scattering from surfaces to see if these theories can explain our results for diamond surfaces. Two different physical processes are discussed in the literature, with publication of

supporting experimental and theoretical work. One concept pertains to metal surfaces and the other to insulating surfaces.

4.1. Charge exchange with metal surfaces

Surface ionization using metal surfaces – and in particular using low WF metal surfaces – is a well-established method developed for fusion plasma research, and a lot of literature is available, e.g. [5,6,7,27]. Briefly, the incoming positive ion is neutralized at a large distance in front of the surface through a resonant transition followed by an Auger de-excitation. Therefore, in the outgoing part of the trajectory only neutral and negatively charged particles have to be considered. In order for a negative ion to be produced the affinity level must be populated with an electron transferred from the surface. The affinity level undergoes a downshift close to the surface because of the interaction with the induced image charge in the metal. To first order this downshift amounts to

$$\Delta E(z)=\frac{q_0^2}{4\pi\,\epsilon_0}\,\frac{1}{4(z-z_S)}, \tag{2}$$

where z is the distance to the surface and z_S is the electrostatic screening length in the metal. Once the position of the affinity level gets close the work function of the metal, resonant one-electron tunneling between the metal and the atom will populate the negative ionic state. Since affinity levels of atoms are of the order of 1 eV, the work function of a metal (usually around 5 eV) has to be lowered by the application of a thin overlayer of an alkali metal or an alkaline earth metal [8] to obtain appreciable yields of negative ions [5,9].

For clean metals electron tunneling does not occur because there are no occupied states close to the affinity level of the atom. However, if the particles are sufficiently fast the population of the negative ion state can proceed via kinetic effects facilitated by the relatively high velocity component parallel to the surface [30,31]. The interplay between electron capture into the affinity state of the atom and electron loss to the conduction band of the surface results in an effective distance of formation, z^*, of the negative ion. The final negative ion yield is dominated by electron loss, thus only modest negative ion yields of the order of 10^{-3} are obtained. The main feature of negative ion formation after grazing incidence scattering (angle $<1°$) from clean metal surfaces is a kinetic resonance with an onset at a velocity perpendicular to the surface around 0.1 a.u. and a maximum yield of a few per mill of 0.5 a.u. [31]. The velocity where the yield of negative ions maximizes is given by

$$v_{\max}=\sqrt{2(\mathrm{WF}-E_A-\Delta E(z^*))}. \tag{3}$$

The negative ion formation is most effective where the largest number of occupied electrons are in resonance with the affinity level E_A [31], with the downshift, $\Delta E(z^*)$, evaluated at the effective distance of formation of the negative ion.

The Fermi edge of the diamond surface is about 5 eV below the vacuum level, which is similar to most of the metals, with the main difference being that the bandgap extends from the Fermi edge up to the vacuum level for the diamond crystal (and even beyond for the (111) surface). If kinetic processes governed the negative ion formation for scattering from diamond, Eq. (3) would predict the maximum negative ion yield to be at velocities of 0.483 a.u. and 0.426 a.u. for the formation of H^- and O^- ions, respectively. Since diamond is an insulator, an important ingredient of the theory of kinetic charge transfer is missing: the electron loss from the ion to the surface. Moreover, the "free electron metal" assumption, another ingredient of the theory, is certainly not fulfilled for diamond. Thus the prediction by Eq. (3) may not be taken that seriously. However, no indication of a kinetic resonance is observed in our measurements where the velocity parallel to the surface ranges from 0.077 a.u. to 0.12 a.u. This is below the onset found for negative ion production for scattering from clean metal surfaces [30,31]. Thus, kinetic processes are most likely not responsible for the formation of negative ions in our case.

4.2. Charge exchange with insulating surfaces

The charge exchange between the surface and the projectile is certainly different when an insulating surface is used. The bandgap of the insulating

surface effectively prevents neutralization once a negative ion state is populated. For scattering oxygen atoms from a LiF surface, O^- fractions of up to 70% have been reported [12]. It was suggested that the electron is picked up by the projectile from the F^- ions from the surface of the lattice in the course of a binary collision. LiF is an ionic crystal and the valence band electrons are located at the fluorine ions. Since in grazing incidence scattering the particle interacts with several surface atoms at comparable distances, the probability of electron transfer to the affinity state increases correspondingly. Once the affinity state is populated, neutralization by tunneling of the electron back to the solid is inhibited, because there are no empty states available due to the large bandgap of the insulator. The dependence of the yield on the parallel velocity also exhibits the clear signature of a kinetic resonance, with an onset at 0.11 a.u. and a maximum negative ion yield at 0.23 a.u., indicating a kinetic charge exchange process. Eq. (3) would predict the maximum to be at a parallel velocity of 0.91 a.u., but the same reservations as above have to be applied to using Eq. (3) for measurements on LiF.

Diamond is also an insulator with a bandgap of 5.47 eV [16]. Like the LiF surface and other wide bandgap compounds, the unreconstructed (hydrogen-terminated) diamond (111) surface exhibits a negative electron affinity, the lower edge of the conduction band being 0.7 eV above the vacuum level [16]. In contrast to LiF, which is an ionic crystal, diamond is entirely covalent. Thus the electrons are not localized at specific sites on the surface and negative ionization is possible at every impact location. Our particles come in at an angle of 8° with respect to the surface. This is much steeper compared to the measurements reported for LiF [12], which were done at grazing angle of incidence (0.5° to 1.5°). In our measurements the interaction of the projectile with the surface will be restricted to only one or very few atoms, and surface channeling will not occur. This compares to the 20 to 70 atoms which contribute to the population of the affinity level when scattering from LiF [12]. The electron transfer has to be much more efficient for diamond than for LiF, because it has to occur in a single impact. As was stated above, no kinetic resonance is observed in our measurements. The velocity range where we observe negative ionization is below the onset for negative ion production for scattering from a LiF surface [12]. Thus, the charge exchange as it is discussed for the LiF surface does not seem to apply for the diamond surface.

The effect of the velocity perpendicular to the surface on the kinetic resonance is small, both on the insulator and on the clean metal surface. It was found that the negative ion yield increases slightly with the velocity perpendicular to the surface, but does not change the shape of the resonance at all [12,31]. The velocities perpendicular to the surface we used are in the same range as these earlier measurements.

The formation of negative ions observed in our experiment appears to be outside the scope of the current theoretical models. Diamond is not a low WF surface and we find no indication for kinetic processes being responsible for the formation of negative ions. We chose diamond as a conversion surface, because we thought that a surface which easily releases electrons into vacuum might also work well for providing an electron to an atom being scattered from its surface. Diamond surfaces are known to be good electron donators facilitated by their low or negative electron affinity (in particular the hydrogen-terminated (111) surface). Our conjecture is that a theory explaining the high yields of negative ions from diamond surfaces will have to include the electron affinity of the surface in some way. Since single crystal diamond coatings of defined orientation are not available at present, we decided to investigate polycrystalline diamond. In the future we plan to use single-crystal diamonds cleaved from natural diamonds. These diamonds have significant nitrogen and boron impurities which change the electronic structure. Type IIb diamond is even a semiconductor. It remains to be seen what effect that has on the formation of negative ions.

5. Conclusions

We have observed the formation of negative ions upon reflection of positively charged particles from

a diamond surface. We showed that the formation of negative ions by surface ionization can be performed despite moderate residual background gas pressure, and can be maintained for extended periods. Elaborate surface preparation does not seem necessary. These are major advantages over the conventional conversion surfaces using Cs or Ba overlayers on metals [6–9], which need elaborate preparation procedures and periodic reconditioning. Moreover, the ionization efficiency of the diamond surface does not degrade upon intense UV irradiation. Since the ionization efficiency remains constant with time for the diamond surface, the incoming neutral particle flux in a space instrument can be measured quantitatively all the time without further diagnostic devices, which is an additional asset for an application on a space platform. All the previously mentioned requirements for the application of a diamond surface for surface ionization in space instrumentation are met.

Diamond has the smallest lattice constant, and the atoms of a diamond crystal are more densely packed than those in any other known material. Therefore, a single-crystal diamond would be an even better surface for particle reflection. Atomically flat and monocrystalline surfaces show not only smaller angular scattering but also a higher particle reflection, i.e. fewer particles are implanted into the converter surface. Thus with a single-crystal diamond surface, we would expect a reduction in the angular width of the scattered beam. The higher particle reflection and narrower angular scattering of a single-crystal surface would enhance the high sensitivity of our instrument, where the expected flux of neutral particles entering the instrument is of the order of tens per second [4].

Acknowledgements

We gratefully acknowledge the free diamond sample provided by Diamonex, Inc. Furthermore, the authors are grateful to J. Fischer, H. Hofstetter and R. Liniger for their contributions in the areas of design, fabrication and electronics, respectively, to Professor P. Bochsler for stimulating discussions, and to Dr. Arthur Ghielmetti for carefully reading the manuscript. This work was supported by the Swiss National Science Foundation.

References

[1] Imager for Magnetopause-to-Aurora Global Exploration (IMAGE), NASA MIDEX program, Principal investigator Dr. James Burch, Southwest Research Institute, San Antonio, TX, USA.

[2] P. Wurz, P. Bochsler, A.G. Ghielmetti, E.G. Shelley, F. Herrero and M.F. Smith, Concept for the HI-LITE neutral atom imaging instrument, Proceedings of the Symposium on Surface Science, Eds. P. Varga and G. Betz, Kaprun, Austria (1993), pp. 225–230.

[3] A.G. Ghielmetti, E.G. Shelley, S. Fuselier, P. Wurz, P. Bochsler, F. Herrero, M.F. Smith and T. Stephen, Mass spectrograph for imaging low energy neutral atoms, Opt. Eng. 33 (1994) 362.

[4] P. Wurz, M.R. Aellig, P. Bochsler, A.G. Ghielmetti, E.G. Shelley, S.A. Fuselier, F. Herrero, M.F. Smith and T.S. Stephen, Neutral atom mass spectrograph, Opt. Eng. 34 (1995) 2365.

[5] J.N.M. van Wunnik, J.J.C. Geerlings, E.H.A. Granneman and J. Los, The scattering of hydrogen atoms from a cesiated tungsten surface, Surf. Sci. 131 (1983) 17.

[6] J.J.C. Geerlings, P.W. van Amersfoort, L.F.Tz. Kwakman, E.H.A. Granneman and J. Los, H^- formation in proton-metal collisions, Surf. Sci. 157 (1985) 151.

[7] J. Los and J.J.C. Geerlings, Charge exchange in atom surface collisions, Phys. Rep. 190 (1990) 133.

[8] N.D. Lang, Theory of work-function changes induced by alkali adsorption, Phys. Rev. B 4 (1971) 4234.

[9] C.F.A. van Os, P.W. Amersfoort and J. Los, Negative ion formation at a barium surface exposed to an intense positive-hydrogen ion beam, J. Appl. Phys. 64 (1988) 3863.

[10] M.R. Aellig, P. Wurz, R. Schletti, P. Bochsler, A.G. Ghielmetti, E.G. Shelley, S. Fuselier, M. Quinn, F. Herrero and M.F. Smith, Surface ionization for space applications, AGU Monograph on Measurement Techniques for Space Plasmas (1996), to be published.

[11] R. Schletti, Master Thesis, University of Bern, Switzerland, 1996.

[12] C. Auth, A.G. Borisov and H. Winter, High fractions of negative ions in grazing scattering of fast oxygen atoms from a LiF(100) surface, Phys. Rev. Lett. 75 (1995) 2292.

[13] M.R. Aellig, Master Thesis, University of Bern, Switzerland, 1995.

[14] Diamonex, Inc., 7150 Windsor Drive, Allentown, PA 18106, USA.

[15] P.G. Lurie and J.M. Wilson, The diamond surface: I. The structure of the clean surface and the interaction with gases and metals, Surf. Sci. 65 (1977) 453.

[16] F.J. Himpsel, J.A. Knapp, J.A. van Vechten and D.E. Eastman, Quantum photoyield of diamond (111) – a stable negative-affinity emitter, Phys. Rev. B 20 (1979) 624.

[17] M.T. Robinson, Slowing-down time of energetic atoms in solids, Phys. Rev. B 40 (1989) 10717.
[18] M. Stix, The Sun (Springer, Berlin, 1991).
[19] F.M. Propst and E. Luescher, Auger electron ejection from tungsten surface by low-energy ions, Phys. Rev. 132 (1963) 1037.
[20] K.J. Snowdon, B. Willerding and W. Heiland, Molecule excitation in sputtering, scattering, and electron or photon induced desorption, Nucl. Instrum. Methods B 14 (1986) 467.
[21] P.J. Schneider, W. Eckstein and H. Verbeek, Charge states of reflected particles for grazing incidence of D^+, D_2^+ and D^0 on Ni and Cs targets, Nucl. Instrum. Methods 194 (1982) 387.
[22] T. Schlathölter and W. Heiland, Charge exchange of swift molecules H_2^+, H_2, CO_2^+ and CO_2, at Pd(111) surfaces, Nucl. Instrum. Methods B 100 (1995) 352.
[23] B. Willerding, W. Heiland and K.J. Snowdon, Neutralization of fast molecular ions H_2^+ and N_2^+ at surfaces, Phys. Rev. Lett. 53 (1984) 2031.
[24] U. van Slooten, D. Andersson and A.W. Kleyn, Scaling law for dissociation of fast molecular hydrogen scattered from Ag(111), Chem. Phys. Lett. 185 (1991) 440.
[25] T.E. Sharp, Potential energy diagram for molecular hydrogen and its ions, Lockheed Palo Alto Research Laboratory, LMSC 5-10-69-9 (1969) 1–84.
[26] R. Schnitzer and M. Anbar, Mechanisms of formation of diatomic and triatomic hydrogen negative ions, J. Chem. Phys. 65 (1976) 1117.
[27] E.H.A. Granneman, J.J.C. Geerlings, J.N.M. van Wunnik, P.J. van Bommel, H.J. Hopman and J. Los, H^- and Li^- formation by scattering H^+, H_2^+, and Li^+ from cesiated tungsten surfaces, Am. Inst. Phys. 243 (1984) 206.
[28] P.H.F. Reijnen, P.J. van den Hoek, A.W. Kleyn, U. Imke and K.J. Snowdon, The O_2–Ag(111) interaction studied by 100–3000 eV glancing incidence O_2^+ scattering, Surf. Sci. 221 (1989) 427.
[29] F.R. Gilmore, Potential energy curves for N_2, NO, O_2 and corresponding ions, J. Quant. Spectrosc. Radiat. Transfer 5 (1965) 369.
[30] H. Winter, Charge transfer in grazing ion–surface scattering, Comm. Mod. Phys. D 26 (1991) 287.
[31] F. Wyputta, R. Zimny and H. Winter, H^- formation in grazing collisions of fast protons with an Al(111) surface, Nucl. Instrum. Methods B 58 (1991) 379.